Sequence Modeling Is Not Evolutionary Reasoning

Yasha Ektefaie* ‡
Department of Biomedical Informatics
Harvard Medical School
Boston, MA 02115
yasha_ektefaie@hms.harvard.edu

Andrew Shen*
Department of Biomedical Informatics
Harvard Medical School
Boston, MA 02115
ashen7@stanford.edu

Lavik Jain
Department of Biomedical Informatics
Harvard Medical School
Boston, MA 02115
lavikjain@college.harvard.edu

Maha Farhat
Department of Biomedical Informatics
Harvard Medical School
Boston, MA 02115
maha_farhat@hms.harvard.edu

Marinka Zitnik ‡
Department of Biomedical Informatics
Harvard Medical School
Boston, MA 02115
marinka@hms.harvard.edu

Abstract

Protein language models (PLMs) are commonly assumed to capture evolutionary information by training on large protein sequence datasets. However, it remains unclear whether PLMs can reason about evolution—that is, infer evolutionary relationships between protein sequences. To test this capability, we introduce a benchmark for evolutionary reasoning and find that existing PLMs consistently fail to recover phylogenetic structure, despite strong performance on standard tasks such as masked token prediction and contact prediction. To address this limitation, we present PHYLA. PHYLA introduces a hybrid state-space and transformer architecture that jointly process multiple sequences and is trained using a tree-based objective over 3,000 phylogenies spanning diverse protein families. PHYLA achieves state-of-the-art performance in evolutionary reasoning, outperforming the next-best model by 13% on tree reconstruction and 10% on taxonomic clustering. Beyond synthetic benchmarks, PHYLA applies to real-world settings: it reconstructs biologically accurate branches of the tree of life and infers whole-genome evolutionary relationships from *Mycobacterium tuberculosis* genomes. These findings suggest that evolutionary reasoning is not an emergent property of large-scale sequence modeling. Instead, PHYLA shows that models trained with phylogenetic supervision can reason about evolution more effectively, offering a biologically grounded path toward evolutionary foundation models.

1 Introduction

Protein language models (PLMs) use transformers with masked language or autoregressive self-supervision to model molecular sequences (Rives et al., 2021; Lin et al., 2022; Alley EC, 2019; Madani, 2023; Notin, 2022). PLMs have shown state-of-the-art performance across predictive (Meier et al., 2021; Rives et al., 2021; Rao et al., 2021; Elnaggar et al., 2021; Alley EC, 2019; Rao et al.,

*Co-first authors, ‡Corresponding

2020) and generative (Lin et al., 2022; Hayes et al., 2024; Madani, 2023; Ferruz, 2022) tasks. At their core, PLMs learn statistical distributions over amino acid sequences, modeling which residues are likely to appear given their surrounding context. This enables powerful zero-shot predictions of mutational effects by observing how the likelihood of a substitution changes under the model. Over time, this paradigm has been framed as a form of "evolutionary modeling," with the assumption that capturing residue-level distributions implicitly reflects evolutionary dynamics.

However, in this work, we argue that this paradigm conflates *evolutionary modeling* with *evolutionary reasoning*. Evolutionary modeling, as practiced by current PLMs, involves capturing local amino acid distributions to estimate residue likelihoods. In contrast, evolutionary reasoning requires a deeper level of abstraction: given a set of sequences, can a model infer the evolutionary relationships that generated them? This includes identifying shared ancestry, relative divergence, and tree-like structure — tasks that cannot be solved by distributional modeling alone.

This distinction is critical. Evolutionary reasoning is the foundation of phylogenetic analysis — a problem that predates modern biology and underlies centuries of effort to reconstruct how life has changed through time. Classical phylogenetics attempts to recover the tree of life Hug (2016) from observed sequences, but current PLMs are not evaluated on their ability to do this. They operate largely in isolation, modeling individual sequences without explicit multi-sequence comparison, structure discovery, or relational inference. Beyond phylogeny, important biological insights can be discerned from reasoning across sequences, whether it is determining the impact of a protein variant (Meier et al., 2021; Brandes, 2023; et al., 2023) or annotating functions of poorly characterized proteins (Nguyen et al., 2024; Avsec, 2021; Zvyagin et al., 2022; Queen et al., 2024)

This work poses the following question: *Are current PLMs capable of evolutionary reasoning? And if not, how must we reimagine their architecture and training to enable them to do so?*

Present Work. To address the limitations of current PLMs in performing evolutionary reasoning, we make several contributions. First, we introduce the first benchmark for evolutionary reasoning over protein sequences, built from curated datasets containing ground-truth phylogenetic trees derived from established phylogenetic studies and databases. This benchmark enables rigorous evaluation of whether models can infer evolutionary structure from sets of sequences, rather than simply modeling local residue distributions. Second, we evaluate existing PLMs on this benchmark. Using their learned embeddings, we attempt to reconstruct phylogenetic trees and find that these models Lin et al. (2022); Hayes et al. (2024); ESM Team (2024); Nijkamp et al. (2022); Brixi et al. (2025) fail to outperform a simple baseline: Hamming distance. This analysis highlights a fundamental limitation: current PLMs are architecturally and functionally optimized for intra-sequence modeling, not inter-sequence reasoning.

To address this gap, we propose PHYLA, a new model architecture designed for evolutionary reasoning. PHYLA is a hybrid state-space and sparsified attention model that processes multiple sequences jointly. It alternates between inter-sequence modules, which detect conserved motifs across sequences, and intra-sequence modules, which contextualize these motifs within individual sequences—allowing the model to reason over sequence sets. We also introduce a novel pretraining objective tailored to phylogenetic structure. Instead of using masked language modeling, PHYLA is trained using a tree loss that teaches the model to embed sequences such that their pairwise distances reflect the correct evolutionary topology.

Despite its compact size (24M parameters), PHYLA achieves state-of-the-art performance in phylogenetic tree reconstruction and competitive accuracy in mutation effect prediction. On TreeBase—a dataset of protein sequences paired with phylogenetic trees from published studies—PHYLA outperforms much larger models, including ESM-3 (1.4B) and ProGen-XLarge (6.4B), by 8.5% and 15.7% respectively, based on normalized Robinson-Foulds (normRF) distance. On the ProteinGym mutation effect prediction benchmark, it achieves a Spearman correlation of 0.6380, matching or exceeding models with several orders of magnitude more parameters. We further demonstrate PHYLA's capacity for evolutionary reasoning by applying it to reconstruct the tree of life from ribosomal protein sequences spanning bacteria, archaea, and eukarya. Additionally, we use PHYLA to infer whole-genome evolutionary relationships among Mycobacterium tuberculosis isolates. In both cases, the resulting trees deviate from canonical topologies and instead reflect known functional distinctions, suggesting that PHYLA learns representations aligned with true biological structure. These results position PHYLA as a foundation for a new generation of protein models grounded in evolutionary reasoning rather than sequence-level pattern recognition alone.

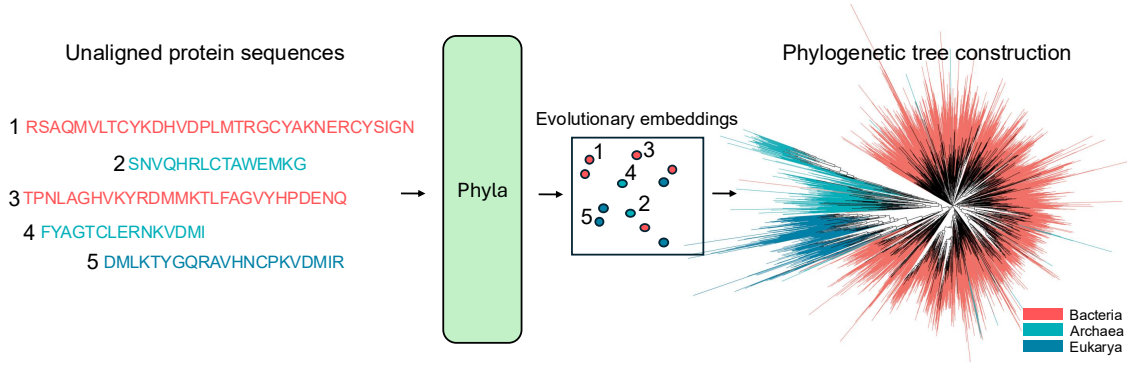

Figure 1: PHYLA takes unaligned protein sequences and generates embeddings that reflects relative evolutionary distance between input sequences which we can use to construct phylogenetic trees.

2 Related Work

Protein Language Models (PLMs). State-of-the-art protein language models include transformer-based models such as ESM2 (Lin et al., 2022), ESMC ESM Team (2024), ProGen (Madani, 2023), and Progen2 Nijkamp et al. (2022) that are trained using masked or autoregressive language modeling. These models learn to model the language of proteins by learning the co-occurrence of amino acid residues within a diverse training set. Other PLMs, such as ESM3 (Hayes et al., 2024), model additional data modalities. ESM3 considers structural and functional information in addition to the background amino acid sequences. These models have demonstrated good performance on intra-sequence reasoning from sequence modeling pre-training tasks but have not explicitly been trained on inter-sequence reasoning between different sequences in the training set.

Alternatives to self-attention. Self-attention is the backbone of the transformer but suffers from quadratic scaling with sequence length, making modeling longer protein sequences difficult (Vaswani et al. (2017)). The Mamba state-space architecture has been proposed as an alternative backbone architecture for sequence-based foundation models. The architecture builds upon the S4 class of structured state-space models (Gu et al. (2022)) by adding a selection mechanism and a hardware-aware parallel algorithm. These advances allow Mamba to model long sequences efficiently. Beyond Mamba, other approaches use similar ideas to extend context length, including Hyena (Poli et al., 2023a) and xLSTM (Beck et al., 2024). More recent work has shown hybrid transformer and attention architectures allow for long-context modeling while maintaining the advantages of transformers Poli et al. (2023b); Ren et al. (2025).

Bioinformatics approaches to phylogenetic analysis. Traditional tree reconstruction methods for a set of input protein sequences consist of generating a multiple sequence alignment (MSA) using one of many alignment algorithms. The MAFFT and Clustal Omega alignment algorithms are popular choices for efficient and accurate MSA generation (Katoh et al. (2002); Sievers et al. (2011)). These alignment algorithms align the input sequences by matching the location of the most conserved amino acids within the sequences. After generating the MSA, a phylogenetic tree is reconstructed using a tree reconstruction algorithm, like FastTree and IQTree (Price et al. (2010); Nguyen et al. (2014)). These algorithms infer the structure of the phylogenetic tree with and without parametric models and usually with various heuristics to generate the most likely phylogenetic tree topology. The primary limitation of tree reconstruction is runtime inefficiency as tree sizes grow. More recent works can be found in the Appendix A.7.

3 Problem Definition

Notation We denote a collection of n protein sequences as $S = \{s_1, s_2, \ldots, s_n\}$, where each s_i is a variable-length sequence over the alphabet Σ of 20 standard amino acids: $\Sigma = \{A, C, \ldots, Y\}$. A phylogenetic tree is denoted by T, with leaves in bijection with S, and subtrees as $t \in T$. The true evolutionary distance between two sequences is denoted $d_{\text{evol}}(i, j)$, and we define $D_{\text{true}} \in \mathbb{R}^{n \times n}$ and $D_{\text{pred}} \in \mathbb{R}^{n \times n}$ as the ground-truth and predicted distance matrices, respectively.

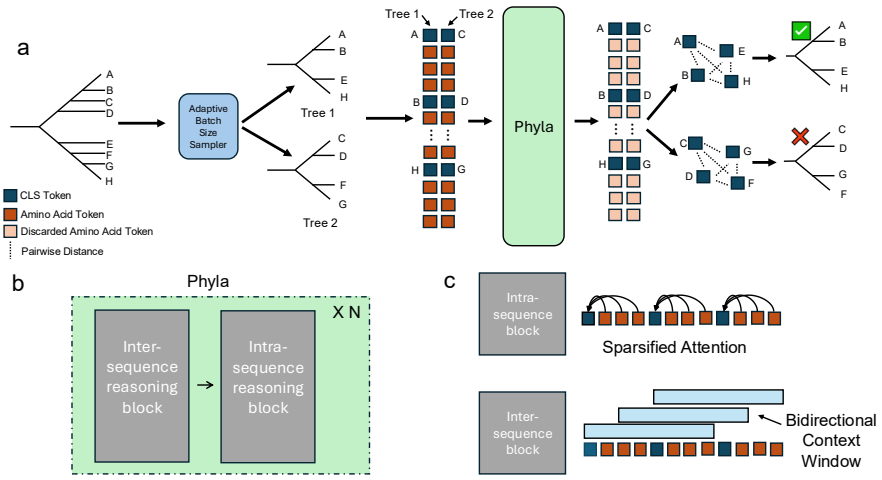

Figure 2: Overview of the PHYLA. (a) PHYLA processes batches of protein sequences sampled from a tree, learning embeddings used to reconstruct phylogenies. (b) It alternates inter- and intra-sequence reasoning blocks. (c) Inter-sequence reasoning uses long bidirectional convolutions to extract shared motifs; intra-sequence reasoning applies sparsified attention to maintain per-sequence context.

Our model PHYLA learns a parametric encoder $f_\theta : \Sigma^* \to \mathbb{R}^d$ that maps each sequence s_i to an embedding $f_\theta(s_i)$. Predicted distances are computed as:

$$D_{ij} = \|f_\theta(s_i) - f_\theta(s_j)\|.$$

We define quartets as 4-tuples of distinct indices (i, j, k, ℓ) drawn from $\{1, \ldots, n\}$, and let $\mathcal{Q}$ be the set of sampled quartets. Each quartet defines three possible unrooted tree topologies: $ij|k\ell$, $ik|j\ell$, and $i\ell|jk$. The temperature parameter T^* controls the sharpness of the softmax logits in quartet loss.

Problem Given a collection of variable-length protein sequences $S = \{s_1, \ldots, s_n\}$, our goal is to reconstruct the latent evolutionary history that generated them, represented as a strictly binary phylogenetic tree T whose leaves correspond to the sequences in S.

To achieve this, we learn a distance-preserving encoder f_θ such that the embedding-based distance $D_{ij} = \|f_\theta(s_i) - f_\theta(s_j)\|$ approximates the true evolutionary distance $d_{\text{evol}}(i, j)$. We then reconstruct T by applying a fast distance-based tree builder to the predicted matrix D_{pred}.

Alignment-Free and Guide-Tree-Free Unlike most prior methods, our approach does not rely on a multiple sequence alignment (MSA) or a predefined guide tree (i.e., a fixed topology to scaffold inference). Removing both introduces new challenges: alignment and tree inference are jointly NP-hard WANG & JIANG (1994); Roch (2005), and guide trees offer strong structural priors. By dispensing with both, PHYLA must discover meaningful patterns directly from unaligned sequences—capturing evolutionary structure without relying on handcrafted heuristics.

4 Methods

4.1 Overview of PHYLA Model Architecture

To do well on evolutionary reasoning, models must be able to perform good inter- and intra-sequence reasoning. **Inter-sequence reasoning** requires the model to detect motifs that recur across different sequences, revealing shared evolutionary signatures. **Intra-sequence reasoning** requires the model to contextualize identified motifs within the context of an individual sequence to determine evolutionary divergence from the identified motif.

To meet these requirements, we introduce a hybrid state-space transformer model, PHYLA. PHYLA alternates between inter-sequence and intra-sequence reasoning blocks. Inter-sequence blocks employ a parameter-efficient state-space module with gated linear recurrence and deep receptive fields,

enabling the model to detect long-range evolutionary motifs across sequences. Intra-sequence blocks then use sparsified attention to contextualize these motifs within each sequence (Appendix A.1.1).

Unlike most PLMs which operate on a single sequence at a time (Lin et al. (2022); Hayes et al. (2024); ESM Team (2024); Notin et al. (2023b); Nijkamp et al. (2022)), **PHYLA is the first PLM designed to process multiple sequences concurrently**. This enables it to directly compare sequences, identify conserved motifs, and exploit these inter-sequence relationships to infer evolutionary structure at inference time. While prior models have employed hybrid state-space transformer architectures (Poli et al. (2023b)), PHYLA introduces a sparsification mechanism: an attention mask M that constrains each token to attend only to tokens within its own sequence, preserving intra-sequence context while enabling efficient multi-sequence processing. Specifically M:

$$M_{ij} = \begin{cases} 1, & \text{if the } j\text{-th token is within the } i\text{-th sequence,} \\ 0, & \text{otherwise.} \end{cases} \tag{1}$$

4.2 Phyla Model Training

Tree Loss Pretraining. To teach PHYLA how to model input sequences to recapitulate evolutionary relationships, we designed a novel tree loss pretraining function. Constructing a phylogenetic tree contains a series of decisions in how to split sequences based on their relative distance to each other. With this in mind, we use a *quartet loss* to supervise training. The quartet loss encourages the model to embed sequences such that inferred distances preserve correct quartet topologies. For a set of n sequences with predicted pairwise distances $D_{\text{pred}} \in \mathbb{R}^{n \times n}$ and true distances $D_{\text{true}} \in \mathbb{R}^{n \times n}$, we sample a set of quartets $\mathcal{Q} = \{(i, j, k, \ell)\}$. For each quartet, we compute three possible pairwise distance sums:

$$\begin{aligned} s_{ij|k\ell} &= D_{ij} + D_{k\ell}, \\ s_{ik|j\ell} &= D_{ik} + D_{j\ell}, \\ s_{i\ell|jk} &= D_{i\ell} + D_{jk}, \end{aligned}$$

and convert them into logits using a softmax-like transformation:

$$\text{logits}_q = \frac{1}{T^*} \left(\begin{bmatrix} s_{ij|k\ell} & s_{ik|j\ell} & s_{i\ell|jk} \end{bmatrix} - \text{mean}(s_{ij|k\ell}, s_{ik|j\ell}, s_{i\ell|jk}) \right),$$

where T^* is a temperature hyperparameter controlling softness. We compute the cross-entropy loss between these logits and the ground-truth minimum sum (from D_{true}):

$$\mathcal{L}_{\text{quartet}} = \frac{1}{|\mathcal{Q}|} \sum_{q \in \mathcal{Q}} \text{CrossEntropy}(\text{logits}_q, \arg \min_{\alpha \in \{ij|k\ell, ik|j\ell, i\ell|jk\}} s_\alpha^{\text{true}}).$$

Quartet loss is the sole pretraining objective used to train PHYLA. **In contrast to most protein language models, which rely on masked language modeling (MLM) over amino acids, PHYLA does not use MLM.**

Training PHYLA. During training, a phylogenetic tree T is sampled, where T consists of N sequences S. Each sequence is tokenized with an alphabet 23 tokens, corresponding to 20 standard amino acids, a CLS token, a mask token, and a pad token. The input to PHYLA is S with a $[CLS]$ token concatenated in front of each tokenized sequence, $s \in S$: $\{[CLS]s_1 \parallel [CLS]s_2 \parallel [CLS]s_3, ..., [CLS]s_n\}$. The size and number of trees considered in each training step are determined at each training step by an adaptive batch size sampler.

We employ an adaptive batch sizing approach to efficiently utilize GPU memory and avoid overfitting to a specific tree topology. We determine the largest subtree $t \in T$ at every training step that can fit within the available GPU memory. Next, we randomly sample a subtree size n such that $10 \leq n \leq |t|$, where $|t|$ is the number of sequences in t. Finally, we identify how many subtrees of the sampled size $|t|$ can be accommodated within the GPU memory. If the model encounters an out-of-memory (OOM) error during this process, the subtrees are resampled with both the subtree size and the number of subtrees halved. Further implementation details are provided in the Appendix A.1.2.

5 Experiments

Datasets. We evaluate PHYLA on a range of evolutionary and functional reasoning tasks. For phylogenetic tree reconstruction, we use two held-out datasets: TreeBase, which includes 1,533 curated phylogenetic trees across diverse species (Piel & Tannen (2009)), and TreeFam, which contains 9,586 gene-family trees spanning a wide evolutionary range (Li et al. (2006)). Dataset statistics are provided in Table 3 and Table 4, with further details in Appendix A.2.1. To assess taxonomic classification, we use bacterial isolate sequences from the Genome Taxonomy Database (GTDB) (Parks et al. (2021)). We define five classification tasks at different levels of taxonomic granularity: Class, Order, Family, Genus, and Species. These tasks measure the model's ability to cluster sequences according to hierarchical evolutionary relationships. Together, these seven tasks—tree reconstruction in TreeBase and TreeFam, and taxonomic classification at five levels using GTDB—form our evolutionary reasoning benchmark. To evaluate performance beyond evolutionary structure, we also assess performance on functional prediction using the ProteinGym benchmark, which consists of 83 protein mutation effect datasets (Notin et al., 2023a) (Appendix A.2.2).

Baselines. We consider four protein language models, one genomic foundation model, six models from the ProteinGym benchmark, and a naive Hamming distance baseline. The protein language models include ESM2, ESM3, ESM C, and ProGen2 (Lin et al. (2022); Hayes et al. (2024); ESM Team (2024); Nijkamp et al. (2022)). The genomic foundation model is Evo 2 (Brixi et al. (2025)). The six models from the ProteinGym benchmark are ProteinNPT, MSA Transformer, ESM-1v, Tranception, TranceptEVE, and DeepSequence (Notin et al. (2023a,b); Rao et al. (2021); Meier et al. (2021); Notin et al. (2022); Riesselman (2018); Notin (2022)).

Evaluation setup. We consider three evaluation settings. **Tree reconstruction**: This setting evaluates the model's ability to reconstruct phylogenetic trees given solely the original sequences. We evaluate tree reconstruction by comparing the predicted tree to the reference tree using the normalized Robinson-Foulds metric (Robinson & Foulds (1981)). **Taxonomic clustering**: This setting evaluates the model's ability to perform fine-grained and coarse-grained classification of sequences. We cluster 500 sequences at each taxonomic level of Class, Order, Family, Genus, and Species and assess the homogeneity of the predicted clusters. **Functional prediction**: This setting evaluates the model's ability to predict functional labels given solely the original sequences. We assess functional prediction by training a linear probe classifier on the generated embeddings, and also by utilizing the predicted tree structure to assign labels. More details can be found in Appendix A.2.1.

5.1 PHYLA can Reason over Protein Sequences

Experimental setup. To assess the ability of PHYLA to reason over sequences, we assess PHYLA's ability to reconstruct phylogenetic trees on the TreeBase and TreeFam datasets. We use the metric of Robinson-Foulds distance, or "RF", whereby a larger RF value is equivalent to a larger distance between predicted and reference tree, and can be interpreted as a lower quality predicted tree. The RF metric is not invariant to tree size, so we compute the normalized RF, or "normRF", to directly compare the tree reconstruction performance between trees of different sizes. We utilize the ETE3 Toolkit implementation of RF and normRF distance (Jaime Huerta-Cepas & Bork (2016)). In addition, we assess PHYLA's ability to cluster sequences across various taxonomic levels. We report the metric of homogeneity across predicted clusters as a measure of the ability to classify sequences. We compare the performance of PHYLA against PLMs (ESM2, ESM3, ESM C, ProGen2) and a genomic foundation model (Evo 2) (Lin et al. (2022); Hayes et al. (2024); ESM Team (2024); Nijkamp et al. (2022); Brixi et al. (2025)). Table 1 shows the normRF performance of PHYLA and benchmark models on the TreeBase and TreeFam datasets.

Results. PHYLA achieves the best performance on both the TreeBase and TreeFam tree reconstruction benchmarks, outperforming all tested baselines—including models with 12 to 266 times more parameters, such as ESM2 (650M) and ProGen2-XLarge (6.4B) (Table 1). On TreeFam, PHYLA reduces normRF by 13.4% compared to the next-best model (ESM2 650M). On the taxonomy clustering benchmark, PHYLA also achieves the best performance across all taxonomic levels, improving species-level homogeneity by 23.2% over the strongest baseline. Notably, all PLMs underperform compared to the naive Hamming distance baseline on TreeBase, highlighting the challenge of this dataset. These results underscore the effectiveness of incorporating evolutionary structure into PHYLA architecture and training.

Table 1: **Evolutionary reasoning benchmark comparing PHYLA to existing protein language models (PLMs).** Tree reconstruction performance on TreeBase and TreeFam is evaluated using normalized Robinson-Foulds distance (normRF), where lower values indicate better agreement with ground truth phylogenies. Clustering performance at the class, order, family, genus, and species levels is measured using homogeneity scores, with higher values indicating more accurate unsupervised grouping according to known taxonomic labels. For other clustering metrics see Appendix A.6.

Model	**TreeBase** ↓	**TreeFam** ↓	**Class** ↑	**Order** ↑	**Family** ↑	**Genus** ↑	**Species** ↑
Hamming Distance	0.7466	0.7509	–	–	–	–	–
ESM2 (650M)	0.7809	0.6669	0.6378	0.6616	0.6838	0.7096	0.7542
ESM2 (3B)	0.7947	0.6729	0.5456	0.5624	0.5688	0.5873	0.6666
ESM3 (1.4B)	0.8139	0.7170	0.6067	0.6314	0.6596	0.6712	0.7212
ESM C (300M)	0.7680	0.7077	0.5743	0.6042	0.6223	0.6684	0.7145
ESM C (600M)	0.7990	0.7252	0.6106	0.6600	0.6577	0.7086	0.7522
Evo 2 (7B)	0.8372	0.8406	0.5002	0.5383	0.5521	0.5511	0.6398
ProGen2-Large (2.7B)	0.7747	0.6752	0.6049	0.6469	0.6641	0.7134	0.7505
ProGen2-XLarge (6.4B)	0.8624	0.8249	0.5157	0.5466	0.5705	0.6130	0.6800
Phyla (24M)	***0.7269***	***0.5777***	***0.7096***	***0.7646***	***0.8749***	***0.9267***	***0.9821***

5.2 PHYLA Trees Encode Protein Functional Information

Experimental setup. To evaluate the expressivity of the learned embeddings from PHYLA, we train a linear probe on predicting functional labels from the embeddings for the baseline methods. We also integrate functional annotations with the constructed trees and utilize the tree structures to infer phenotypic labels to evaluate whether the trees generated by PHYLA encode meaningful biological information. To generate functional predictions from tree structure, we overlay functional labels from the train sequences onto the tree. Next, local sequence clusters are located using TreeCluster (Balaban M (2019)), which assigns cluster membership to each sequence in the evaluation set. Finally, the predicted functional label for a test sample within a certain cluster is assigned by calculating the average of the training sample labels within that cluster. We then calculate the spearman rank correlation between predicted and real values as the final metric. We utilize the 83 datasets from the ProteinGym (Notin et al. (2023a)) benchmark as our evaluation set (Appendix A.2.2). Figure 3 shows the average Spearman correlation metric with both the dataset size (in number of sequences trained on) and the model size (in parameters) on the 83 ProteinGym evaluation datasets.

Results. PHYLA achieves competitive performance on the ProteinGym benchmark, ranking among the top-performing models across the 83 functional prediction tasks (Figure 3). Despite being trained on only 34 times less data and with 27 times fewer parameters than models like ESM2 (650M), PHYLA achieves a comparable Spearman correlation of 0.638. Notably, PHYLA outperforms several larger PLMs, including ESM3 (1.4B) and Tranception, demonstrating that its tree-based representations encode meaningful biological function. These results suggest that the structured embeddings produced by PHYLA not only capture phylogenetic and taxonomic information but also generalize to downstream functional prediction—despite minimal model size and data requirements.

5.3 Ablation Analyses

Experimental setup. To understand the effect of the tree loss versus traditional masked langauge modeling loss, we trained PHYLA with only masked language modeling loss (PHYLA-MLM). To probe the effect of PHYLA architecture on performance, we ablated the sparsification attention layers, the intra-sequence reasoning blocks (PHYLA-NoAttention). We then evaluated both ablated PHYLA models on the tree reasoning benchmark and on functional prediction.

Results. As shown in Table 2, pretraining on a masked language modeling (MLM) objective resulted in substantial performance degradation across all tasks: a 19.6% increase in normalized Robinson-Foulds (normRF) distance for tree reconstruction (TreeBase), a 13.2% drop in Spearman correlation for functional prediction (ProteinGym), and a 5.5% reduction in average taxonomic clustering homogeneity. Similarly, ablating sparsified attention led to even greater degradation: a 20.6% increase in normRF, a 31.4% drop in functional prediction, and a 7.3% reduction in taxonomic

Figure 3: **Functional prediction performance on ProteinGym with model sizes and dataset sizes.** Spearman correlation of existing PLMs and PHYLA on ProteinGym benchmark as a function of pretraining dataset size. Model points are sized based on the number of parameters in the model.

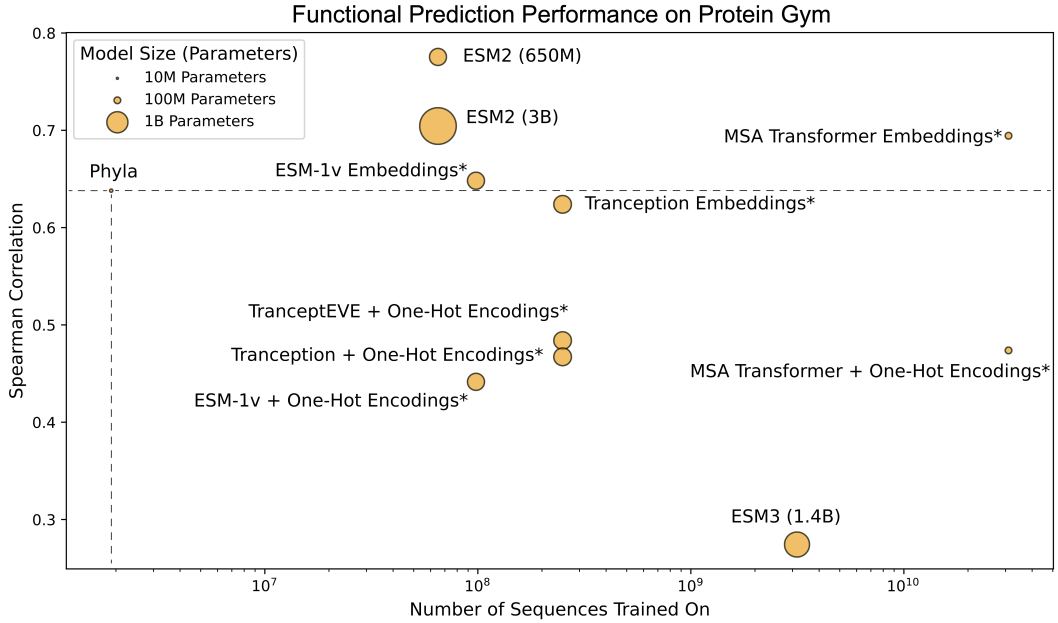

Table 2: **Ablation study on PHYLA's architecture and training objectives.** Tree reconstruction is evaluated on TreeBase and TreeFam using normalized Robinson-Foulds distance (normRF), where lower values indicate better alignment with ground truth trees. Functional prediction is assessed on ProteinGym using Spearman correlation (higher is better). Taxonomic clustering is evaluated at five hierarchical levels—class, order, family, genus, and species—using homogeneity scores, with higher values indicating more taxonomically consistent clusters. Additional clustering metrics are reported in Appendix A.5.

Model	**TreeBase** ↓	**TreeFam** ↓	**ProteinGym** ↑	**Class** ↑	**Order** ↑	**Family** ↑	**Genus** ↑	**Species** ↑
PHYLA-MLM	0.8291	0.7892	0.5536	0.6613	0.7554	0.8028	0.8712	0.9495
PHYLA-NoAttention	0.8556	0.7839	0.4377	0.6929	0.7427	0.7830	0.8227	0.9192
PHYLA	***0.7269***	***0.5777***	***0.6380***	***0.7096***	***0.7646***	***0.8749***	***0.9267***	***0.9821***

clustering. These results highlight that both the tree-based training objective and the sparsified attention mechanism are critical to PHYLA's overall performance. In contrast, relying solely on MLM pretraining without architectural or objective innovations significantly harms phylogenetic, taxonomic, and functional understanding.

5.4 PHYLA application to real world datasets

PHYLA demonstrates promising performance in sequence reasoning. To showcase its capabilities, we applied PHYLA to the task of phylogenetic tree construction. The tree of life is a fundamental framework in biology, delineating evolutionary relationships between organisms and serving as an indicator of relative phenotypic traits. Current approaches to constructing the tree of life typically rely on multiple sequence alignments of ribosomal proteins (Hug et al., 2016). We used PHYLA to analyze a set of 3,084 phylogenetic sequences, successfully reconstructing the tree of life in just 16 hours, compared to the 3,840 hours required by traditional methods (Hug et al., 2016) (Appendix A.3).

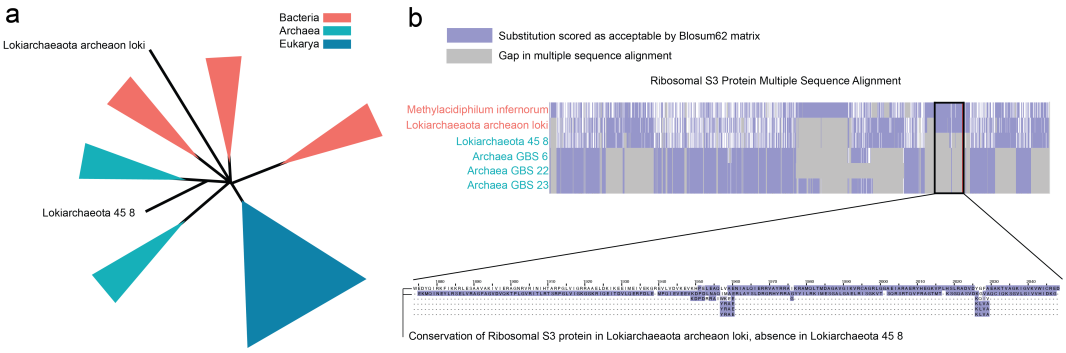

Figure 4: **PHYLA created a new placement of Lokiarchaea.** a. Lokiarchaeaota archeaon loki (L-A) was placed among bacterial neighbors while Lokiarchaeota 45 8 (L-45) was placed among archaeal neighbors. b. Analysis of the multiple sequence alignment revealed that L-A placed with bacteria retained a conserved S3 ribosomal protein, aligning with its bacterial neighbors. In contrast, the L-45 placed with archaea exhibited a deletion of the S3 ribosomal protein, aligning with its archaeal neighbors.

As shown in Figure 1, PHYLA accurately places sequences within their respective domains in the tree of life. PHYLA identifies overlap between certain archaeal isolates and bacteria, a result consistent with current phylogenetic reasoning. Lokiarchaeota, an archaeal lineage clustered with bacteria, is known to have a mosaic genome with over 30% of its genome derived from bacteria (Levasseur et al., 2017). Within this genus, Phyla placed Lokiarchaeaota archaeon loki (L-A) paraphyletic to bacteria while Lokiarchaeota 45 8 (L-45) is paraphyletic to archaea (Figure 4a). Examination of the multiple sequence alignment of L-45 and L-A with their immediate phylgenetic neighbors, revealed that L-45 harbors a deletion of the S3 ribosomal protein while L-A retains this protein (Figure 4b). The S3 deletion has been noted in previous studies of Lokiarchaea genomes Da Cunha et al. (2017). Biologically, these differences may relate to adaptation to extreme environments. L-45 was isolated from the bottom of the Arctic Ocean, while L-A was isolated from the Horonobe Underground Research Laboratory (URL) in Japan. In fact, L-A's neighbor, Methylacidiphilum infernorum, is an acidophilic methanotroph originally isolated from a geothermal area in New Zealand Hou et al. (2008). This environment shares similarities with the conditions in the URL, where extensive methane metabolism has been observed Amano et al. (2024). This highlights PHYLA's ability to discover potentially biologically meaningful evolutionary relationships. We also apply PHYLA to whole-genome sequences of Mycobacterium tuberculosis, aligning over 4 megabases of DNA to infer novel phylogenetic relationships among clinical isolates (Appendix A.4).

6 Conclusion

We introduced an evolutionary reasoning benchmark and showed that existing protein language models (PLMs) struggle to capture evolutionary structure, indicating their latent spaces do not reflect phylogenetic relationships among sequences. To address this gap, we proposed PHYLA, a hybrid state-space transformer trained with a novel tree-based loss function. PHYLA achieves state-of-the-art performance on the evolutionary reasoning benchmark, while also performing competitively on functional prediction tasks—despite being trained on 34 times less data and with 27 times fewer parameters than models like ESM2 650M. Ablation studies confirmed that evolutionary reasoning does not emerge from sequence modeling alone and requires explicit inductive bias. Limitations and future directions are discussed in Appendix A.8.

Competing Interests

The authors declare no competing interests.

Code Availability Statement

Code to run Phyla can be found in the project github.

References

Gustaf Ahdritz, Nazim Bouatta, Sachin Kadyan, Lukas Jarosch, Daniel Berenberg, Ian Fisk, Andrew M. Watkins, Stephen Ra, Richard Bonneau, and Mohammed AlQuraishi. Openproteinset: Training data for structural biology at scale, 2023. URL https://arxiv.org/abs/2308.05326.

Biswas S AlQuraishi M Church GM Alley EC, Khimulya G. Unified rational protein engineering with sequence-based deep representation learning. *Nat Methods*, 2019. doi: 10.1038/s41592-019-0598-1.

Stephen F Altschul, Warren Gish, Webb Miller, Eugene W Myers, and David J Lipman. Basic local alignment search tool. *Journal of molecular biology*, 215(3):403–410, 1990.

Yusuke Amano, Rishabh Sachdeva, Daniel Gittins, Karthik Anantharaman, Shuwei Lei, Laura E. Valentin-Alvarado, Samuel Diamond, Hiroshi Beppu, Teruki Iwatsuki, Ayako Mochizuki, Keiko Miyakawa, Eri Ishii, Hiroshi Murakami, Adam L. Jaffe, Cindy Castelle, Adi Lavy, Yohei Suzuki, and Jillian F. Banfield. Diverse microbiome functions, limited temporal variation and substantial genomic conservation within sedimentary and granite rock deep underground research laboratories. *Environmental Microbiome*, 19(1):105, Dec 2024. doi: 10.1186/s40793-024-00649-3.

Agarwal V. Visentin D. et al. Avsec, Ž. Effective gene expression prediction from sequence by integrating long-range interactions. *Nature Methods*, 2021. doi: 10.1038/s41592-021-01252-x. URL https://www.nature.com/articles/s41592-021-01252-x.

Mai U Jia X Mirarab S Balaban M, Moshiri N. Treecluster: Clustering biological sequences using phylogenetic trees. *PLoS ONE. 14(8):e0221068*, 2019. doi: 10.1371/journal.pone.0221068.

Maximilian Beck, Korbinian Pöppel, Markus Spanring, Andreas Auer, Oleksandra Prudnikova, Michael Kopp, Günter Klambauer, Johannes Brandstetter, and Sepp Hochreiter. xlstm: Extended long short-term memory, 2024. URL https://arxiv.org/abs/2405.04517.

Goldman G. Wang C.H. et al. Brandes, N. Genome-wide prediction of disease variant effects with a deep protein language model. *Nature Genetics*, 2023. doi: 10.1038/s41588-023-01465-0. URL https://www.nature.com/articles/s41588-023-01465-0.

Garyk Brixi, Matthew G. Durrant, Jerome Ku, Michael Poli, Greg Brockman, Daniel Chang, Gabriel A. Gonzalez, Samuel H. King, David B. Li, Aditi T. Merchant, Mohsen Naghipourfar, Eric Nguyen, Chiara Ricci-Tam, David W. Romero, Gwanggyu Sun, Ali Taghibakshi, Anton Vorontsov, Brandon Yang, Myra Deng, Liv Gorton, Nam Nguyen, Nicholas K. Wang, Etowah Adams, Stephen A. Baccus, Steven Dillmann, Stefano Ermon, Daniel Guo, Rajesh Ilango, Ken Janik, Amy X. Lu, Reshma Mehta, Mohammad R.K. Mofrad, Madelena Y. Ng, Jaspreet Pannu, Christopher Ré, Jonathan C. Schmok, John St. John, Jeremy Sullivan, Kevin Zhu, Greg Zynda, Daniel Balsam, Patrick Collison, Anthony B. Costa, Tina Hernandez-Boussard, Eric Ho, Ming-Yu Liu, Thomas McGrath, Kimberly Powell, Dave P. Burke, Hani Goodarzi, Patrick D. Hsu, and Brian L. Hie. Genome modeling and design across all domains of life with evo 2. *bioRxiv*, 2025. doi: 10.1101/2025.02.18.638918. URL https://www.biorxiv.org/content/early/2025/02/21/2025.02.18.638918.

Violette Da Cunha, Morgan Gaia, Daniele Gadelle, Arshan Nasir, and Patrick Forterre. Lokiarchaea are close relatives of euryarchaeota, not bridging the gap between prokaryotes and eukaryotes. *PLoS Genet.*, 13(6):e1006810, June 2017.

Xian Ding, Zijun Zou, and Charles L. Brooks III. Deciphering protein evolution and fitness landscapes with latent space models. *Nature Communications*, 10:5644, 2019. doi: 10.1038/s41467-019-13633-0. URL https://doi.org/10.1038/s41467-019-13633-0.

Ahmed Elnaggar, Michael Heinzinger, Christian Dallago, Ghalia Rihawi, Yu Wang, Llion Jones, Tom Gibbs, Tamas Feher, Christoph Angerer, Martin Steinegger, Debsindhu Bhowmik, and Burkhard Rost. Prottrans: Towards cracking the language of life's code through self-supervised deep learning and high performance computing, 2021. URL https://arxiv.org/abs/2007.06225.

ESM Team. Esm cambrian: Revealing the mysteries of proteins with unsupervised learning, 2024. URL https://evolutionaryscale.ai/blog/esm-cambrian.

J. Cheng et al. Accurate proteome-wide missense variant effect prediction with alphamissense. *Science*, 2023. doi: 10.1126/science.adg7492. URL https://www.science.org/doi/10.1126/science.adg7492.

Schmidt S. Höcker B. Ferruz, N. Protgpt2 is a deep unsupervised language model for protein design. *Nature Communications*, 2022. doi: 10.1038/s41467-022-32007-7. URL https://www.nature.com/articles/s41467-022-32007-7.

Jonathan Frazer, Pascal Notin, Mafalda Dias, Aidan Gomez, Joseph K Min, Kelly P. Brock, Yarin Gal, and Debora S. Marks. Disease variant prediction with deep generative models of evolutionary data. *Nature*, 2021.

Lorenzo Freschi, Ronald Vargas, Amna Husain, et al. Population structure, biogeography and transmissibility of *Mycobacterium tuberculosis*. *Nature Communications*, 12:6099, 2021. doi: 10.1038/s41467-021-26248-1. URL https://doi.org/10.1038/s41467-021-26248-1.

Albert Gu, Karan Goel, and Christopher Ré. Efficiently modeling long sequences with structured state spaces, 2022. URL https://arxiv.org/abs/2111.00396.

Thomas Hayes, Roshan Rao, Halil Akin, Nicholas J. Sofroniew, Deniz Oktay, Zeming Lin, Robert Verkuil, Vincent Q. Tran, Jonathan Deaton, Marius Wiggert, Rohil Badkundri, Irhum Shafkat, Jun Gong, Alexander Derry, Raul S. Molina, Neil Thomas, Yousuf Khan, Chetan Mishra, Carolyn Kim, Liam J. Bartie, Matthew Nemeth, Patrick D. Hsu, Tom Sercu, Salvatore Candido, and Alexander Rives. Simulating 500 million years of evolution with a language model. *bioRxiv*, 2024. doi: 10.1101/2024.07.01.600583. URL https://www.biorxiv.org/content/early/2024/07/02/2024.07.01.600583.

Shaobin Hou, Kira S Makarova, Jimmy H W Saw, Pavel Senin, Benjamin V Ly, Zhemin Zhou, Yan Ren, Jianmei Wang, Michael Y Galperin, Marina V Omelchenko, Yuri I Wolf, Natalya Yutin, Eugene V Koonin, Matthew B Stott, Bruce W Mountain, Michelle A Crowe, Angela V Smirnova, Peter F Dunfield, Lu Feng, Lei Wang, and Maqsudul Alam. Complete genome sequence of the extremely acidophilic methanotroph isolate v4, methylacidiphilum infernorum, a representative of the bacterial phylum verrucomicrobia. *Biol. Direct*, 3:26, July 2008.

Baker B. Anantharaman K. et al. Hug, L. A new view of the tree of life. *Nature Microbiology*, 2016. doi: 10.1038/nmicrobiol.2016.48. URL https://www.nature.com/articles/nmicrobiol201648.

Laura A Hug, Brett J Baker, Karthik Anantharaman, Christopher T Brown, Alexander J Probst, Cindy J Castelle, Cristina N Butterfield, Alex W Hernsdorf, Yuki Amano, Kotaro Ise, Yohey Suzuki, Natasha Dudek, David A Relman, Kari M Finstad, Ronald Amundson, Brian C Thomas, and Jillian F Banfield. A new view of the tree of life. *Nat. Microbiol.*, 1:16048, April 2016.

Francois Serra Jaime Huerta-Cepas and Peer Bork. Ete 3: Reconstruction, analysis and visualization of phylogenomic data. *Mol Biol Evol*, 2016. doi: 10.1093/molbev/msw046.

Yueyu Jiang, Metin Balaban, Qiyun Zhu, and Siavash Mirarab. Depp: Deep learning enables extending species trees using single genes. *Systematic Biology*, 72(1):17–34, 04 2022. ISSN 1063-5157. doi: 10.1093/sysbio/syac031. URL https://doi.org/10.1093/sysbio/syac031.

Kazutaka Katoh, Kazuharu Misawa, Kei-ichi Kuma, and Takashi Miyata. Mafft: a novel method for rapid multiple sequence alignment based on fast fourier transform. *Nucleic Acids Research*, 30 (14):3059–3066, 07 2002. ISSN 0305-1048. doi: 10.1093/nar/gkf436. URL https://doi.org/10.1093/nar/gkf436.

Anthony Levasseur, Vicky Merhej, Emeline Baptiste, Vikas Sharma, Pierre Pontarotti, and Didier Raoult. The rhizome of lokiarchaeota illustrates the mosaicity of archaeal genomes. *Genome Biol. Evol.*, 9(10):2635–2639, October 2017.

Heng Li, Avril Coghlan, Jue Ruan, Lachlan James Coin, Jean-Karim Hériché, Lara Osmotherly, Ruiqiang Li, Tao Liu, Zhang Zhang, Lars Bolund, Gane Ka-Shu Wong, Weimou Zheng, Paramvir Dehal, Jun Wang, and Richard Durbin. Treefam: a curated database of phylogenetic trees of animal gene families. *Nucleic Acids Research*, 34(suppl$_1$) : $D572 - -D580, 012006. ISSN0305 - 1048. doi : .$ URL https://doi.org/10.1093/nar/gkj118.

Zeming Lin, Halil Akin, Roshan Rao, Brian Hie, Zhongkai Zhu, Wenting Lu, Nikita Smetanin, Allan dos Santos Costa, Maryam Fazel-Zarandi, Tom Sercu, Sal Candido, et al. Language models of protein sequences at the scale of evolution enable accurate structure prediction. *bioRxiv*, 2022.

Ilya Loshchilov and Frank Hutter. Decoupled weight decay regularization, 2019. URL https://arxiv.org/abs/1711.05101.

Krause B. Greene E.R. et al. Madani, A. Large language models generate functional protein sequences across diverse families. *Nat Biotechnol 41, 1099–1106*, 2023. 10.1038/s41587-022-01618-2.

Aritra Mahapatra and Jayanta Mukherjee. Deephy: A deep learning model to reconstruct phylogenetic tree from unaligned nucleotide sequences. *bioRxiv*, 2025. 10.1101/2025.03.09.642239. URL https://www.biorxiv.org/content/early/2025/03/13/2025.03.09.642239.

Maximillian G Marin, Natalia Quinones-Olvera, Christoph Wippel, Mahboobeh Behruznia, Brendan M Jeffrey, Michael Harris, Brendon C Mann, Alex Rosenthal, Karen R Jacobson, Robin M Warren, Heng Li, Conor J Meehan, and Maha R Farhat. Pitfalls of bacterial pan-genome analysis approaches: a case study of m. tuberculosis and two less clonal bacterial species. *Bioinformatics*, pp. btaf219, 05 2025. ISSN 1367-4811. 10.1093/bioinformatics/btaf219. URL https://doi.org/10.1093/bioinformatics/btaf219.

Joshua Meier, Roshan Rao, Robert Verkuil, Jason Liu, Tom Sercu, and Alexander Rives. Language models enable zero-shot prediction of the effects of mutations on protein function. *bioRxiv*, 2021. 10.1101/2021.07.09.450648. URL https://www.biorxiv.org/content/early/2021/07/10/2021.07.09.450648.

Takahiro Mimori and Michiaki Hamada. Geophy: Differentiable phylogenetic inference via geometric gradients of tree topologies, 2023. URL https://arxiv.org/abs/2307.03675.

Luca Nesterenko, Luc Blassel, Philippe Veber, Bastien Boussau, and Laurent Jacob. Phyloformer: Fast, accurate, and versatile phylogenetic reconstruction with deep neural networks. *Molecular Biology and Evolution*, 42(4):msaf051, 03 2025. ISSN 1537-1719. 10.1093/molbev/msaf051. URL https://doi.org/10.1093/molbev/msaf051.

Eric Nguyen, Michael Poli, Matthew G. Durrant, Armin W. Thomas, Brian Kang, Jeremy Sullivan, Madelena Y. Ng, Ashley Lewis, Aman Patel, Aaron Lou, Stefano Ermon, Stephen A. Baccus, Tina Hernandez-Boussard, Christopher Ré, Patrick D. Hsu, and Brian L. Hie. Sequence modeling and design from molecular to genome scale with evo. *bioRxiv*, 2024. 10.1101/2024.02.27.582234. URL https://www.biorxiv.org/content/early/2024/03/06/2024.02.27.582234.

Lam-Tung Nguyen, Heiko A. Schmidt, Arndt von Haeseler, and Bui Quang Minh. Iq-tree: A fast and effective stochastic algorithm for estimating maximum-likelihood phylogenies. *Molecular Biology and Evolution*, 32(1):268–274, 11 2014. ISSN 0737-4038. 10.1093/molbev/msu300. URL https://doi.org/10.1093/molbev/msu300.

Erik Nijkamp, Jeffrey Ruffolo, Eli N. Weinstein, Nikhil Naik, and Ali Madani. Progen2: Exploring the boundaries of protein language models, 2022. URL https://arxiv.org/abs/2206.13517.

Dias M. Frazer J. Marchena-Hurtado J. Gomez A. Marks D.S. Gal Y. Notin, P. Tranception: Protein fitness prediction with autoregressive transformers and inference-time retrieval. *ICML*, 2022.

Pascal Notin, Lood Van Niekerk, Aaron W Kollasch, Daniel Ritter, Yarin Gal, and Debora S. Marks. Trancepteve: Combining family-specific and family-agnostic models of protein sequences for improved fitness prediction. *bioRxiv*, 2022. 10.1101/2022.12.07.519495. URL https://www.biorxiv.org/content/early/2022/12/10/2022.12.07.519495.

Pascal Notin, Aaron W. Kollasch, Daniel Ritter, Lood van Niekerk, Steffanie Paul, Hansen Spinner, Nathan Rollins, Ada Shaw, Ruben Weitzman, Jonathan Frazer, Mafalda Dias, Dinko Franceschi, Rose Orenbuch, Yarin Gal, and Debora S. Marks. Proteingym: Large-scale benchmarks for protein design and fitness prediction. *bioRxiv*, 2023a. 10.1101/2023.12.07.570727. URL https://www.biorxiv.org/content/early/2023/12/08/2023.12.07.570727.

Pascal Notin, Ruben Weitzman, Debora S. Marks, and Yarin Gal. Proteinnpt: Improving protein property prediction and design with non-parametric transformers. *bioRxiv*, 2023b.

10.1101/2023.12.06.570473. URL https://www.biorxiv.org/content/early/2023/12/07/2023.12.06.570473.

Donovan H Parks, Maria Chuvochina, Christian Rinke, Aaron J Mussig, Pierre-Alain Chaumeil, and Philip Hugenholtz. Gtdb: an ongoing census of bacterial and archaeal diversity through a phylogenetically consistent, rank normalized and complete genome-based taxonomy. *Nucleic Acids Research*, 50(D1):D785–D794, 09 2021. ISSN 0305-1048. 10.1093/nar/gkab776. URL https://doi.org/10.1093/nar/gkab776.

William R. Pearson. An introduction to sequence similarity ("homology") searching. *Current Protocols in Bioinformatics*, Chapter 3:3.1.1–3.1.8, 2013. 10.1002/0471250953.bi0301s42.

Chan L. Dominus M. J. Ruan J. Vos R. A. Piel, W. H. and V. Tannen. Treebase v. 2: A database of phylogenetic knowledge. *e-BioSphere*, 2009.

Michael Poli, Stefano Massaroli, Eric Nguyen, Daniel Y Fu, Tri Dao, Stephen Baccus, Yoshua Bengio, Stefano Ermon, and Christopher Re. Hyena hierarchy: Towards larger convolutional language models. In Andreas Krause, Emma Brunskill, Kyunghyun Cho, Barbara Engelhardt, Sivan Sabato, and Jonathan Scarlett (eds.), *Proceedings of the 40th International Conference on Machine Learning*, volume 202 of *Proceedings of Machine Learning Research*, pp. 28043–28078. PMLR, 23–29 Jul 2023a. URL https://proceedings.mlr.press/v202/poli23a.html.

Michael Poli, Jue Wang, Stefano Massaroli, Jeffrey Quesnelle, Ryan Carlow, Eric Nguyen, and Armin Thomas. StripedHyena: Moving Beyond Transformers with Hybrid Signal Processing Models, 12 2023b. URL https://github.com/togethercomputer/stripedhyena.

Morgan N. Price, Paramvir S. Dehal, and Adam P. Arkin. Fasttree 2 – approximately maximum-likelihood trees for large alignments. *PLOS ONE*, 5(3):1–10, 03 2010. 10.1371/journal.pone.0009490. URL https://doi.org/10.1371/journal.pone.0009490.

Owen Queen, Yepeng Huang, Robert Calef, Valentina Giunchiglia, Tianlong Chen, George Dasoulas, LeAnn Tai, Yasha Ektefaie, Ayush Noori, Joseph Brown, et al. Procyon: A multimodal foundation model for protein phenotypes. *bioRxiv*, pp. 2024–12, 2024.

Roshan Rao, Joshua Meier, Tom Sercu, Sergey Ovchinnikov, and Alexander Rives. Transformer protein language models are unsupervised structure learners. *bioRxiv*, 2020. 10.1101/2020.12.15.422761. URL https://www.biorxiv.org/content/early/2020/12/15/2020.12.15.422761.

Roshan M Rao, Jason Liu, Robert Verkuil, Joshua Meier, John Canny, Pieter Abbeel, Tom Sercu, and Alexander Rives. Msa transformer. In Marina Meila and Tong Zhang (eds.), *Proceedings of the 38th International Conference on Machine Learning*, volume 139 of *Proceedings of Machine Learning Research*, pp. 8844–8856. PMLR, 18–24 Jul 2021. URL https://proceedings.mlr.press/v139/rao21a.html.

Liliang Ren, Yang Liu, Yadong Lu, yelong shen, Chen Liang, and Weizhu Chen. Samba: Simple hybrid state space models for efficient unlimited context language modeling. In *The Thirteenth International Conference on Learning Representations*, 2025. URL https://openreview.net/forum?id=bIlnpVM4bc.

Ingraham J.B. Marks D.S. Riesselman, A.J. Deep generative models of genetic variation capture the effects of mutations. *Nature Method*, 2018. 10.1038/s41592-018-0138-4. URL https://www.nature.com/articles/s41592-018-0138-4.

Alexander Rives, Joshua Meier, Tom Sercu, Siddharth Goyal, Zeming Lin, Jason Liu, Demi Guo, Myle Ott, C. Lawrence Zitnick, Jerry Ma, and Rob Fergus. Biological structure and function emerge from scaling unsupervised learning to 250 million protein sequences. *Proceedings of the National Academy of Sciences*, 118(15):e2016239118, 2021. 10.1073/pnas.2016239118. URL https://www.pnas.org/doi/abs/10.1073/pnas.2016239118.

D.F. Robinson and L.R. Foulds. Comparison of phylogenetic trees. *Mathematical Biosciences*, 53(1):131–147, 1981. ISSN 0025-5564. https://doi.org/10.1016/0025-5564(81)90043-2. URL https://www.sciencedirect.com/science/article/pii/0025556481900432.

S. Roch. A short proof that phylogenetic tree reconstruction by maximum likelihood is hard, 2005. URL https://arxiv.org/abs/math/0504378.

Yair Schiff, Chia-Hsiang Kao, Aaron Gokaslan, Tri Dao, Albert Gu, and Volodymyr Kuleshov. Caduceus: Bi-directional equivariant long-range dna sequence modeling, 2024. URL https://arxiv.org/abs/2403.03234.

Fabian Sievers, Andreas Wilm, David Dineen, Toby J Gibson, Kevin Karplus, Weizhong Li, Rodrigo Lopez, Hamish McWilliam, Michael Remmert, Johannes Söding, Julie D Thompson, and Desmond G Higgins. Fast, scalable generation of high-quality protein multiple sequence alignments using clustal omega. *Molecular Systems Biology*, 7(1):539, 2011. https://doi.org/10.1038/msb.2011.75. URL https://www.embopress.org/doi/abs/10.1038/msb.2011.75.

Jason Thorpe, Wipaporn Sawaengdee, Danielle Ward, et al. Multi-platform whole genome sequencing for tuberculosis clinical and surveillance applications. *Scientific Reports*, 14:5201, 2024. 10.1038/s41598-024-55865-1. URL https://doi.org/10.1038/s41598-024-55865-1.

Ashish Vaswani, Noam Shazeer, Niki Parmar, Jakob Uszkoreit, Llion Jones, Aidan N. Gomez, Łukasz Kaiser, and Illia Polosukhin. Attention is all you need. In *Proceedings of the 31st International Conference on Neural Information Processing Systems*, NIPS'17, pp. 6000–6010, Red Hook, NY, USA, 2017. Curran Associates Inc. ISBN 9781510860964.

LUSHENG WANG and TAO JIANG. On the complexity of multiple sequence alignment. *Journal of Computational Biology*, 1(4):337–348, 1994. 10.1089/cmb.1994.1.337. URL https://doi.org/10.1089/cmb.1994.1.337. PMID: 8790475.

Eli Weinstein, Alan Amin, Jonathan Frazer, and Debora Marks. Non-identifiability and the blessings of misspecification in models of molecular fitness. In S. Koyejo, S. Mohamed, A. Agarwal, D. Belgrave, K. Cho, and A. Oh (eds.), *Advances in Neural Information Processing Systems*, volume 35, pp. 5484–5497. Curran Associates, Inc., 2022. URL https://proceedings.neurips.cc/paper_files/paper/2022/file/247e592848391fe01f153f179c595090-Paper-Conference.pdf.

World Health Organization. Global tuberculosis report 2024, 2024. URL https://www.who.int/publications/i/item/9789240101531. Licence: CC BY-NC-SA 3.0 IGO.

Tianyu Xie and Cheng Zhang. Artree: A deep autoregressive model for phylogenetic inference. In *Advances in Neural Information Processing Systems*, volume 36, 2023. Spotlight.

Tianyu Xie, Harry Richman, Jiansi Gao, Frederick A. Matsen, and Cheng Zhang. Phylovae: Unsupervised learning of phylogenetic trees via variational autoencoders. In *Proceedings of the International Conference on Learning Representations (ICLR)*, Jan 2025. Accepted as Poster.

Maxim Zvyagin, Alexander Brace, Kyle Hippe, Yuntian Deng, Bin Zhang, Cindy Orozco Bohorquez, Austin Clyde, Bharat Kale, Danilo Perez-Rivera, Heng Ma, Carla M. Mann, Michael Irvin, J. Gregory Pauloski, Logan Ward, Valerie Hayot, Murali Emani, Sam Foreman, Zhen Xie, Diangen Lin, Maulik Shukla, Weili Nie, Josh Romero, Christian Dallago, Arash Vahdat, Chaowei Xiao, Thomas Gibbs, Ian Foster, James J. Davis, Michael E. Papka, Thomas Brettin, Rick Stevens, Anima Anandkumar, Venkatram Vishwanath, and Arvind Ramanathan. Genslms: Genome-scale language models reveal sars-cov-2 evolutionary dynamics. *bioRxiv*, 2022. 10.1101/2022.10.10.511571. URL https://www.biorxiv.org/content/early/2022/10/11/2022.10.10.511571.

A Technical Appendices and Supplementary Material

Table 3: Table that shows information about the 1,533 TreeBase datasets used.

Dataset Metric	Min	Mean	Max	Standard Deviation
Average Sequence Length	5.0	322.4	3658.0	287.7
Number of Sequences	4.0	53.1	1284.0	65.1

Table 4: Table that shows information about the 9,586 TreeFam datasets used.

Dataset Metric	Min	Mean	Max	Standard Deviation
Average Sequence Length	40.0	599.1	31926.0	686.8
Number of Sequences	1.0	32.5	375.0	33.7

A.1 Phyla model architecture and training details

A.1.1 Model architecture details

The PHYLA architecture alternates between inter-sequence and intra-sequence reasoning blocks. Inter-sequence reasoning is performed using BiMamba layers, while intra-sequence reasoning is handled by sparsified attention layers Schiff et al. (2024). The current 24M-parameter PHYLA model comprises three inter-sequence blocks, each containing 16 BiMamba layers followed by a single sparsified attention layer. Each layer operates with a hidden dimension of 256.

A.1.2 Training details

PHYLA was trained on 3,321 high-quality multiple sequence alignments (MSAs) curated from the OpenProteinSet Ahdritz et al. (2023). Low-quality MSAs were removed using the filtering procedure described in EVE Frazer et al. (2021). For each MSA, we compute pairwise distances between sequences by counting the number of matching positions and dividing by the total alignment length. These normalized pairwise distances are used as supervision during training. We used MSA distances and not tree distances because the OpenProteinSet comprised of curated MSAs with no trees. To create trees we would have to run an algorithm on top of the MSA which could introduce biases while training.

The current model has 24M parameters and was trained on 1 80GB H100 GPU for 3 days with the AdamW optimizer using a 10,000 step linear warmup up to a learning rate of 1e-5 (Loshchilov & Hutter (2019)).

Adaptive Batch Size Sampling. We empirically determined that PHYLA can process input lengths up to 213,350 tokens on a 32 GB GPU and up to 302,350 tokens on a 48 GB GPU. For other GPU memory sizes, we used a linear model to estimate the maximum allowable input length. Given the length of the longest protein in the input, we computed the maximum number of sequences that could fit within the memory limit. To reduce overfitting, we randomly sampled the number of sequences between 5 and this maximum. Based on the sampled number of sequences, we then computed the largest batch size that would fit in memory. If a training step triggered an out-of-memory error, we automatically retried with both the number of sequences and the batch size reduced by half.

A.2 Tree reasoning and protein gym benchmark

A.2.1 Tree reasoning benchmark

Tree Reconstruction. We evaluate tree reconstruction performance using two external datasets: TreeBase Piel & Tannen (2009) and TreeFam Li et al. (2006). TreeBase is a curated repository of 12,817 phylogenetic trees from peer-reviewed studies, along with associated sequence data contributed by users. After filtering for trees with complete and parseable sequence information, we retained

1,533 trees for analysis. TreeFam is a database of gene family trees focused on animal genomes. We extracted 9,586 gene trees along with their corresponding protein sequences. For each method, we generated protein embeddings, computed pairwise distances between embeddings, and reconstructed trees using the neighbor-joining algorithm. To evaluate reconstruction quality, we computed the normalized Robinson-Foulds distance (lower is better) between the predicted and reference trees. We found that PHYLA had the lowest normalized Robinson-Foulds distance among all models. This difference was significant ($p < 0.05$, one-sided t-test, Table 5) for all models.

Table 5: P-values from paired t-tests comparing Phyla with baseline models on normalized Robinson-Foulds scores for TreeBase and TreeFam. Lower values indicate statistically significant improvements.

Baseline Model	**TreeBase P-value**	**TreeFam P-value**
ESM2 (650M)	6.78×10^{-16}	1.54×10^{-102}
ESMC (300M)	1.69×10^{-9}	7.95×10^{-222}
ESMC (600M)	4.61×10^{-27}	7.16×10^{-288}
ESM2 (3B)	7.72×10^{-24}	3.95×10^{-118}
ProGen2-Large (2.7B)	1.37×10^{-12}	4.63×10^{-112}
ProGen2-XLarge (6.4B)	7.99×10^{-99}	1.37×10^{-308}
ESM3 (1.4B)	3.20×10^{-40}	5.41×10^{-249}
Evo2 (7B)	4.71×10^{-65}	1.37×10^{-308}

Taxonomic Clustering Evaluation. We evaluate taxonomic structure using data from the Genome Taxonomy Database (GTDB), a high-quality and frequently updated resource for microbial taxonomy. GTDB taxonomic labels are derived by concatenating multiple sequence alignments of 120 marker proteins per organism. We use Release 10-RS226 (released April 16, 2025), which contains 715,230 organisms.

To construct our evaluation dataset, we randomly sample 50 groups of 10 organisms each, ensuring that all organisms within a group share the same taxonomic label at either the class, order, family, genus, or species level depending on the benchmark. For each model, we compute organism-level embeddings as follows: (1) For baseline models, we embed each of the 120 marker proteins independently, then average the resulting embeddings to produce a single vector per organism. (2) For PHYLA, we batch all 500 organisms for each marker protein (e.g., protein 1) and compute embeddings jointly. We repeat this for all 120 proteins, then average across them to obtain organism-level embeddings. We then perform k-means clustering (as implemented in scikit-learn) with k=50, corresponding to the number of groups.

In the main text, we report results for one such sample of 500 organisms. However, we find that performance is consistent across clustering metrics (completeness, homogeneity, NMI) and across random seeds. We generate four additional random samples and report mean and standard deviation across these replicates. Phyla achieves state-of-the-art performance in taxonomic clustering across all taxonomic levels. It is only outperformed by ProGen2-XLarge in completeness at the class level (Table 6).

Table 6: Clustering evaluation metrics (mean ± std) across taxonomic levels. Standard deviation and mean across 5 random taxonomic group samples from GTDB.

Taxonomic Level	Model	Homogeneity	Completeness	NMI
Class	ESM2 (650M)	0.536 ± 0.052	0.638 ± 0.038	0.582 ± 0.045
	ESM3 (1.4B)	0.674 ± 0.010	0.713 ± 0.014	0.693 ± 0.011
	ESMC (300M)	0.547 ± 0.097	0.622 ± 0.096	0.582 ± 0.097
	ESMC (600M)	0.505 ± 0.017	0.592 ± 0.018	0.545 ± 0.017
	ProGen2-Large (2.7B)	0.665 ± 0.023	0.743 ± 0.017	0.702 ± 0.020
	ProGen2-XLarge (6.4B)	0.655 ± 0.039	**0.746 ± 0.025**	0.697 ± 0.033
	Evo2 (7B)	0.583 ± 0.016	0.671 ± 0.009	0.624 ± 0.013
	Phyla	**0.689 ± 0.024**	0.725 ± 0.020	**0.706 ± 0.022**
Family	ESM2 (650M)	0.574 ± 0.045	0.683 ± 0.043	0.623 ± 0.044
	ESM3 (1.4B)	0.745 ± 0.024	0.784 ± 0.025	0.764 ± 0.024
	ESMC (300M)	0.591 ± 0.111	0.671 ± 0.097	0.628 ± 0.105
	ESMC (600M)	0.479 ± 0.041	0.614 ± 0.040	0.538 ± 0.041
	ProGen2-Large (2.7B)	0.735 ± 0.038	0.808 ± 0.030	0.770 ± 0.034
	ProGen2-XLarge (6.4B)	0.652 ± 0.068	0.758 ± 0.050	0.701 ± 0.060
	Evo2 (7B)	0.621 ± 0.051	0.716 ± 0.051	0.665 ± 0.051
	Phyla (24M)	**0.851 ± 0.020**	**0.878 ± 0.015**	**0.865 ± 0.017**
Genus	ESM2 (650M)	0.638 ± 0.053	0.736 ± 0.039	0.683 ± 0.047
	ESM3 (1.4B)	0.825 ± 0.017	0.851 ± 0.020	0.837 ± 0.018
	ESMC (300M)	0.654 ± 0.099	0.727 ± 0.109	0.688 ± 0.104
	ESMC (600M)	0.511 ± 0.088	0.664 ± 0.061	0.576 ± 0.080
	ProGen2-Large (2.7B)	0.774 ± 0.058	0.849 ± 0.041	0.810 ± 0.050
	ProGen2-XLarge (6.4B)	0.675 ± 0.078	0.788 ± 0.051	0.726 ± 0.067
	Evo2 (7B)	0.735 ± 0.059	0.801 ± 0.040	0.767 ± 0.050
	Phyla (24M)	**0.953 ± 0.015**	**0.968 ± 0.011**	**0.960 ± 0.013**
Order	ESM2 (650M)	0.572 ± 0.034	0.674 ± 0.030	0.619 ± 0.032
	ESM3 (1.4B)	0.724 ± 0.029	0.760 ± 0.024	0.741 ± 0.026
	ESMC (300M)	0.580 ± 0.095	0.652 ± 0.103	0.614 ± 0.098
	ESMC (600M)	0.514 ± 0.031	0.631 ± 0.021	0.567 ± 0.027
	ProGen2-Large (2.7B)	0.677 ± 0.043	0.760 ± 0.035	0.716 ± 0.040
	ProGen2-XLarge (6.4B)	0.648 ± 0.026	0.745 ± 0.030	0.693 ± 0.027
	Evo2 (7B)	0.598 ± 0.050	0.694 ± 0.031	0.643 ± 0.042
	Phyla (24M)	**0.779 ± 0.027**	**0.810 ± 0.021**	**0.794 ± 0.024**
Species	ESM2 (650M)	0.685 ± 0.050	0.789 ± 0.037	0.733 ± 0.045
	ESM3 (1.4B)	0.851 ± 0.031	0.882 ± 0.026	0.866 ± 0.029
	ESMC (300M)	0.730 ± 0.055	0.819 ± 0.021	0.771 ± 0.039
	ESMC (600M)	0.523 ± 0.036	0.717 ± 0.039	0.604 ± 0.037
	ProGen2-Large (2.7B)	0.845 ± 0.035	0.899 ± 0.025	0.871 ± 0.029
	ProGen2-XLarge (6.4B)	0.726 ± 0.038	0.830 ± 0.031	0.774 ± 0.034
	Evo2 (7B)	0.816 ± 0.028	0.874 ± 0.025	0.844 ± 0.027
	Phyla (24M)	**0.983 ± 0.007**	**0.992 ± 0.004**	**0.987 ± 0.005**

A.2.2 ProteinGym benchmark

The 83 ProteinGym datasets were chosen based on the memory constraint of a single 80GB H100 GPU. We stratified performance on the ProteinGym functional prediction benchmark across various levels of overlap between pre-training and evaluation datasets. We quantified overlap by running the Basic Local Alignment Search Tool (BLAST) algorithm between each representative sequence of the 83 ProteinGym datasets and each model's pre-training dataset (Altschul et al. (1990)). Overlap was calculated as the average percent similarity of output hits. We did not include the total number of hits

Table 7: **Functional Prediction Across Various Overlap Settings.** Model performance on predicting functional effects in ProteinGym stratified into low-overlap and high-overlap settings based on alignment overlap.

Model	Low-Overlap	High-Overlap	All Datasets
ESM2	0.5863	**0.8013**	**0.7754**
PHYLA-MLM	0.5277	0.6135	0.5535
PHYLA-NoAttention	0.3981	0.5297	0.4377
PHYLA	***0.6208***	*0.6778*	*0.6380*

when calculating the overlap metric in order to not further penalize models with larger pre-training datasets.

When comparing functional prediction performance between PHYLA and ESM2 on all 83 ProteinGym datasets, ESM2 significantly outperforms PHYLA by 0.137. However, on low-overlap regimes with less than 40% similarity to the model's pre-training dataset, PHYLA outperforms ESM2 by 0.034 as shown in Table 7 (Pearson (2013). Performance degrades on low-overlap regimes for all models, but PHYLA's performance degrades less. In addition, PHYLA occupies a lower overlap regime than ESM2, which is likely due to the smaller pre-training set used for PHYLA.

A.3 Tree of Life analysis

To reconstruct the tree of life, we use a dataset of 3,083 organisms, each represented by the concatenated multiple sequence alignment (MSA) of 16 conserved ribosomal proteins Hug (2016). For input to PHYLA, we concatenate the raw amino acid sequences of all 16 ribosomal proteins per organism, yielding sequence lengths of approximately 6 million tokens. We process these sequences using PHYLA on a high-memory CPU machine (800 GB RAM), requiring approximately 16 hours of compute time for a full forward pass. We then compute pairwise distances between organism-level embeddings and apply the neighbor-joining algorithm to construct the resulting phylogenetic tree.

A.4 Tuberculosis analysis

Tuberculosis (TB) is one of the leading causes of death globally due to infectious disease World Health Organization (2024). A major challenge in controlling TB is its capacity to rapidly evolve drug resistance. Genomic surveillance has become a critical tool in addressing this issue: by tracking the evolutionary dynamics of TB, we can detect emerging resistance before it becomes widespread and adapt treatment strategies accordingly Thorpe et al. (2024). We use Phyla to construct the first whole-genome phylogenetic tree of Mycobacterium tuberculosis isolates. Specifically, we analyze 92 complete TB genomes (4 Mb each) Marin et al. (2025). To generate organism-level representations, we divide each genome into non-overlapping 500 bp segments (shared across all 92 genomes), embed each chunk using Phyla, and then average the resulting embeddings across the genome. This approach is well-suited to TB, which is a highly clonal organism with limited variation across isolates—making direct genome chunking and alignment across samples both feasible and meaningful Freschi et al. (2021). We compute pairwise distances between the organism-level embeddings and reconstruct the phylogenetic tree using the neighbor-joining algorithm (Figure 5).

PHYLA successfully clusters Mycobacterium tuberculosis isolates according to their known lineages, including correctly grouping isolates from Lineage 4 and Lineage 2 Freschi et al. (2021). The tree also reflects known ambiguity between Lineages 2 and 3, a pattern previously reported in the TB phylogenetics literature Freschi et al. (2021). However, PHYLA places Lineage 4 closer to Lineage 2 than expected. In established phylogenies, Lineage 4 is believed to have diverged earlier, suggesting a discrepancy from the accepted evolutionary history of TB. This deviation may result from artifacts introduced during genome chunking, or it may point to a previously unrecognized evolutionary signal. Investigating the cause of this discrepancy—and whether it reflects a biological insight or a modeling artifact—is an important direction for future work.

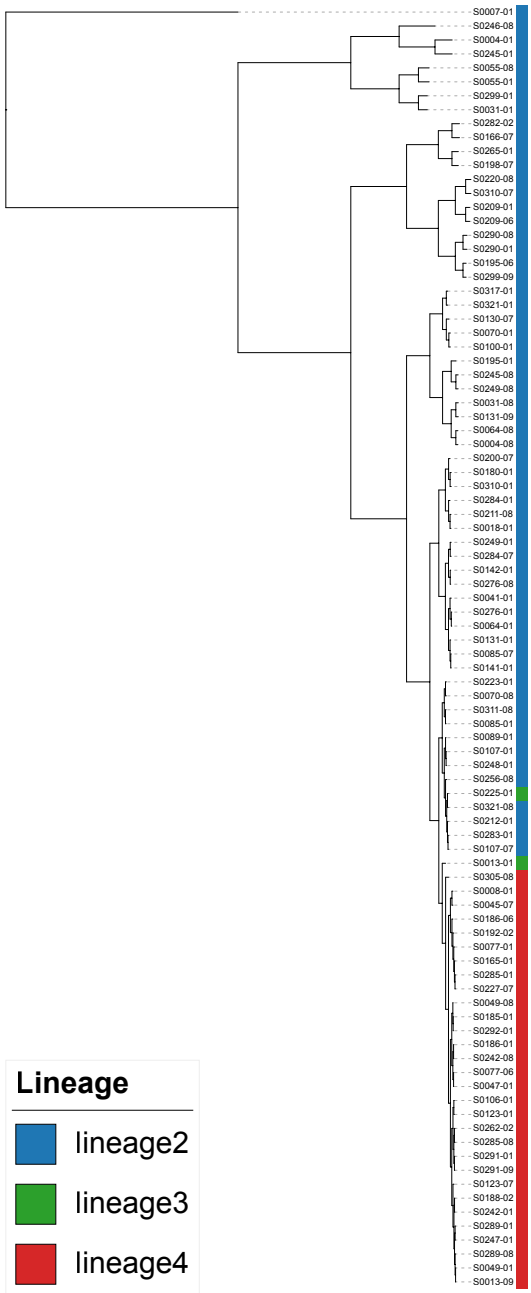

Figure 5: **Phyla generated tree of whole genome Tuberuclosis (TB) isolates.** By comparing chunks of the genome of TB across 92 TB isolates, Phyla constructed the first-whole genome tree of TB. Labeled are the main lineages of TB (lineage2, lineage 3, and lineage 4).

A.5 Ablations

We retested our ablations, Phyla-MLM trained with only the MLM loss and Phyla-NoAttention trained without sparsified attention, on the extended taxonomic clustering dataset described in Section A.2.1. We found across all taxonomic levels, except class, PHYLA had the best performance across all metrics assessed. PHYLA also has significantly better tree reconstruction in TreeBase and TreeFam than all ablations (Table 9).

Table 8: Clustering evaluation metrics (mean ± std) for Phyla variants across taxonomic levels. Standard deviation and mean across 5 random taxonomic group samples from GTDB.

Taxonomic Level	Model	Homogeneity	Completeness	NMI
Class	Phyla-MLM	0.651 ± 0.018	0.686 ± 0.021	0.668 ± 0.019
	Phyla-NoAttention	**0.690 ± 0.018**	**0.740 ± 0.011**	**0.714 ± 0.015**
	Phyla	0.689 ± 0.024	0.725 ± 0.020	0.706 ± 0.022
Family	Phyla-MLM	0.775 ± 0.022	0.804 ± 0.017	0.789 ± 0.019
	Phyla-NoAttention	0.790 ± 0.022	0.831 ± 0.019	0.810 ± 0.021
	Phyla	**0.851 ± 0.020**	**0.878 ± 0.015**	**0.865 ± 0.017**
Genus	Phyla-MLM	0.891 ± 0.016	0.915 ± 0.015	0.903 ± 0.016
	Phyla-NoAttention	0.849 ± 0.029	0.881 ± 0.024	0.865 ± 0.026
	Phyla	**0.953 ± 0.015**	**0.968 ± 0.011**	**0.960 ± 0.013**
Order	Phyla-MLM	0.739 ± 0.014	0.778 ± 0.012	0.758 ± 0.012
	Phyla-NoAttention	0.736 ± 0.029	0.787 ± 0.016	0.761 ± 0.023
	Phyla	**0.779 ± 0.027**	**0.810 ± 0.021**	**0.794 ± 0.024**
Species	Phyla-MLM	0.944 ± 0.011	0.963 ± 0.013	0.954 ± 0.012
	Phyla-NoAttention	0.924 ± 0.011	0.943 ± 0.011	0.934 ± 0.010
	Phyla	**0.983 ± 0.007**	**0.992 ± 0.004**	**0.987 ± 0.005**

Table 9: P-values from paired t-tests comparing Phyla with Phyla ablations on normalized Robinson-Foulds scores for TreeBase and TreeFam. Lower p-values indicate stronger statistical significance.

Baseline Model	TreeBase P-value	TreeFam P-value
PHYLA-MLM	1.14×10^{-57}	0.0
PHYLA-NoAttention	1.94×10^{-91}	0.0

A.6 Evolution Reasoning Result

Please see Section A.2.1.

A.7 Recent Work

Evolutionary reasoning versus evolutionary modeling. Previous studies distinguish between fitting a generative model to observed sequence data and reasoning about the underlying fitness landscape that produced those sequences Weinstein et al. (2022); Ding et al. (2019). From these works, we know generative sequence models aim to match the marginal distribution of extant proteins (evolutionary modeling), whereas evolutionary reasoning seeks to recover the selective pressures and functional constraints driving those distributions.

AI for Phylogenetic Tree Construction. Recent years have seen a surge of AI-driven approaches for evolutionary-biology problems. For instance, PhyloVAE and ARTree Xie et al. (2025); Xie & Zhang (2023) generate plausible tree topologies from collections of existing phylogenies. GeoPhy and Phyloformer Mimori & Hamada (2023); Nesterenko et al. (2025) take an input multiple-sequence alignment (MSA) and infer both tree topology and branch lengths by maximizing the likelihood under a fixed substitution model. Other methods—such as DEPP and DeePhy Jiang et al. (2022); Mahapatra & Mukherjee (2025)—are designed to place unaligned query sequences into a reference phylogenetic tree or into existing triplets of sequences. In contrast, PHYLA focuses on a task that combines these capabilities: starting from unaligned sequences alone, it simultaneously infers a complete tree topology without requiring any prior alignment.

A.8 Limitations and Future Directions

A primary limitation of our approach is its reliance on an external distance-based algorithm (e.g., neighbor-joining) for tree reconstruction. While this may introduce biases, we apply the same reconstruction procedure across all models to ensure fair comparison. Additionally, because PHYLA operates in Euclidean space, it may be suboptimal for modeling hierarchical structures that are more naturally represented in non-Euclidean (e.g., hyperbolic) spaces. Incorporating hyperbolic embeddings into future versions of PHYLA may further enhance its performance. Finally, while we benchmarked against simple baselines such as Hamming distance, we did not compare PHYLA to the full suite of classical phylogenetic pipelines. This choice was deliberate: PHYLA is not intended as a drop-in replacement for existing phylogenetic methods, but rather as a first step toward a new paradigm for evolutionary reasoning with protein language models. Beyond hyperbolic embeddings, future work includes moving away from tree reconstruction with the neighbor-joining algorithm and having PHYLA construct its own tree topologies based on the protein embeddings it generates.

Societal Impacts and Safety Concerns. Our method's ability to generalize beyond its training distribution can lead to more accurate identification of disease-causing variants in previously unseen protein families, potentially accelerating both basic research and the development of personalized therapeutics. However, because this is the first model that infers a phylogenetic tree directly from raw sequence data, there is a risk that users may overestimate its reliability and substitute it for established, alignment-based pipelines. Such overreliance could produce misleading evolutionary hypotheses or clinical interpretations if the model's assumptions and limitations are not carefully considered. To mitigate these dangers, we stress that our approach is intended as a complement to—rather than a replacement for—traditional phylogenetic methods, and that any high-stakes decisions (e.g., in clinical genomics) should always include orthogonal validation.